12

Physical parameters of electrostatic accelerated microparticles

© O.M. Marchenko, S.A. Bednyakov, S.S. Avtorin, O.B. Dzagurov, N.B. Akimov, O.P. Glotov, N.G. Chechenin

Skobeltsyn Institute of Nuclear Physics, Moscow State University, Moscow, Russia
E-mail: oleg.marchenko.99@bk.ru

Received June 30, 2025
Revised August 18, 2025
Accepted August 18, 2025

A system has been launched at the Moscow State University Research Institute of Nuclear Physics based on an electrostatic injector and accelerator, which makes it possible to produce a beam of accelerated metal microparticles with speeds up to 3 km/s. As part of the system, a hardware and software complex has been developed that implements a time-of-flight technique for recording the values of the physical parameters of each individual particle. The distributions of the physical parameters of accelerated particles of two different aluminum powders are obtained.

Keywords: solid particle accelerator, electrostatic injector, macrometeorites, charge-sensitive amplifier.

DOI: 10.61011/TPL.2025.11.62217.20420

Alongside with cosmic radiation, space dust and micrometeoroids rank among the key factors of destructive influence on spacecraft components. The most susceptible to such influence are the optical elements of spacecraft and parts of scientific instruments and solar cells. The average velocity of spacecraft collisions with such particles is on the order of 20 km/s. In the vicinity of the Moon, the typical velocity of dust particles does not exceed the Moon's escape velocity, which is 2.4 km/s. This is attributable to the fact that the concentration of secondary high-velocity particles injected from the surface as a result of meteorite bombardment exceeds the concentration of external high-velocity particles. The size of most particles falls within the range of $1-1000\,\mu$m; smaller particles are effectively removed from the Solar System by light pressure, while larger ones are significantly less common.

Laboratory modeling of the influence of high-velocity microparticles on devices and materials is fraught with significant difficulties. These are associated, on the one hand, with the construction of a system for accelerating particles in the desired direction and, on the other hand, with monitoring of the physical parameters of accelerated particles. Nevertheless, the extremely high cost of flight tests necessitates research into these problems. Among the important objectives of such research are testing and calibration of sensors for measuring the microparticle fluxes in space. These sensors are used in current space missions [1] and are being developed actively in Russia [2–4] for subsequent installation aboard spacecraft. To improve the reliability of such devices and conduct functional testing, one needs to maintain and revise existing laboratory test stands and create new ones.

Electrostatic acceleration is one of the most efficient methods for production of high-velocity microparticles. It involves obtaining individual charged particles from a neutral powder with the use of an electrostatic injector [5] and subsequent acceleration in an electrostatic field. In most cases, a Van de Graaff generator serves as the field source [6,7]. Electrostatic accelerators designed to work with charged microparticles are in operation in the United States and China [8,9]. They are currently used to investigate the influence of accelerated particles on sensor components [10,11], and the obtained results verify the necessity of development of such experimental methods. New methods for accelerating microparticles are also being developed [12]. Studies into the electrostatic acceleration of microparticles have been carried out at the Skobeltsyn Institute of Nuclear Physics (SINP) since the late 1960s [13,14].

The most important component of a system for electrostatic acceleration of charged microparticles is the source of charged microparticles (electrostatic injector). The diagram of the injector used at SINP is shown in Fig. 1.

The dash-and-dot line in Fig. 1 represents the possible path of a particle inside the injector, and asterisks indicate charge exchange events. A particle escaping randomly through one of apertures *5* ends up in the outer chamber of the injector. A bundle of conductive carbon fibers is mounted opposite the outlet aperture on the charging electrode. This is needed to reduce the radius of curvature of the charging electrode surface in the final (prior to escaping from the injector) charge exchange event and to increase the specific charge of a particle. The injector is secured to the vacuum system at the high-voltage terminal of the accelerator through holes in base plate *9*, which also serves as a vacuum flange.

In continuation of earlier research [13,14], a test stand for microparticle acceleration was designed at SINP based on an EG-8 accelerator and an electrostatic injector. The diagram of the setup is shown in Fig. 2. The test stand includes a vacuum system consisting of forevacuum and turbomolecular pumps and a vacuum chamber for the materials or devices under examination. It operates in concert with a hardware and software complex that records the velocities and charges of each passing particle.

The mentioned complex features two sets consisting of a copper detector cylinder and a calibrated charge-sensitive

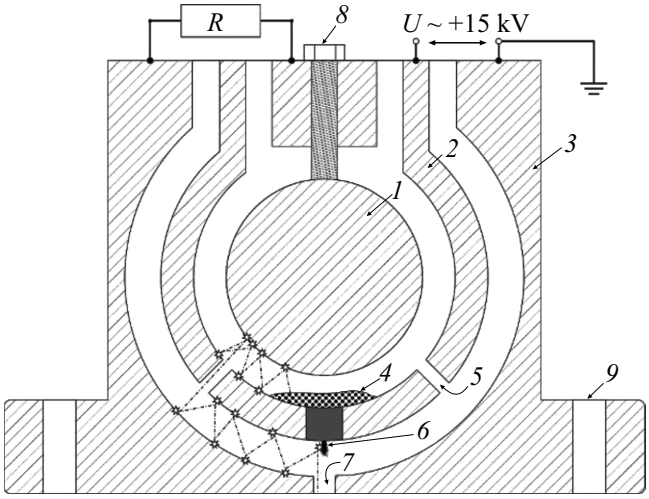


Figure 1. Schematic diagram of the used electrostatic charged particle injector. *1* — Hopper electrode, *2* — charging electrode, *3* — injector body, *4* — powder sample, *5* — aperture between the hopper and the outer chamber, *6* — directed bundle of carbon fibers, *7* — outlet aperture, *8* — adjustment screw, and *9* — injector base.

amplifier (CSA). An AKIP-72204A digital storage eight-bit oscilloscope (with a bandwidth up to 10 MHz), the PicoScope 6 oscilloscope software, and proprietary software for processing the received signals are also used. The general form of signals obtained during measurements is shown in the right part of Fig. 2. The parameters being recorded are the relative times of maxima, minima, and crossing of the baseline voltage at the CSA outputs. Subsequent signal processing provides an opportunity to determine the physical parameters of particles in measurements with two cylinders; knowing the distance between the cylinders and the CSA gain factors, one may calculate the velocity and charge of the particle inducing the pulses in the following manner:

$$v = \frac{L}{\Delta t}, \qquad q = k\frac{1}{2}\Delta U, \tag{1}$$

where v is the particle velocity, L is the distance between the centers of cylinders, Δt is the time interval between the points where the signal crosses the baseline in two channels of the oscilloscope, q is the particle charge, k is the CSA gain factor, and ΔU is the difference between the maximum and minimum voltage values at the CSA output.

The particle mass may then be calculated as

$$\frac{mv^2}{2} = Eq, \qquad m = 2\frac{Eq}{v^2}, \tag{2}$$

where m is the particle mass and E is the total accelerating voltage.

Thus, measurements of the physical parameters of a particle (including its mass, charge, and velocity) are indirect. The error in measured values of the specified parameters is specified primarily by errors in determining the quantities found in formulae (1) and (2) that are not measured directly in the discussed experiment. These include the accelerating voltage, the distance between the cylinders, the geometric dimensions of the cylinders, the

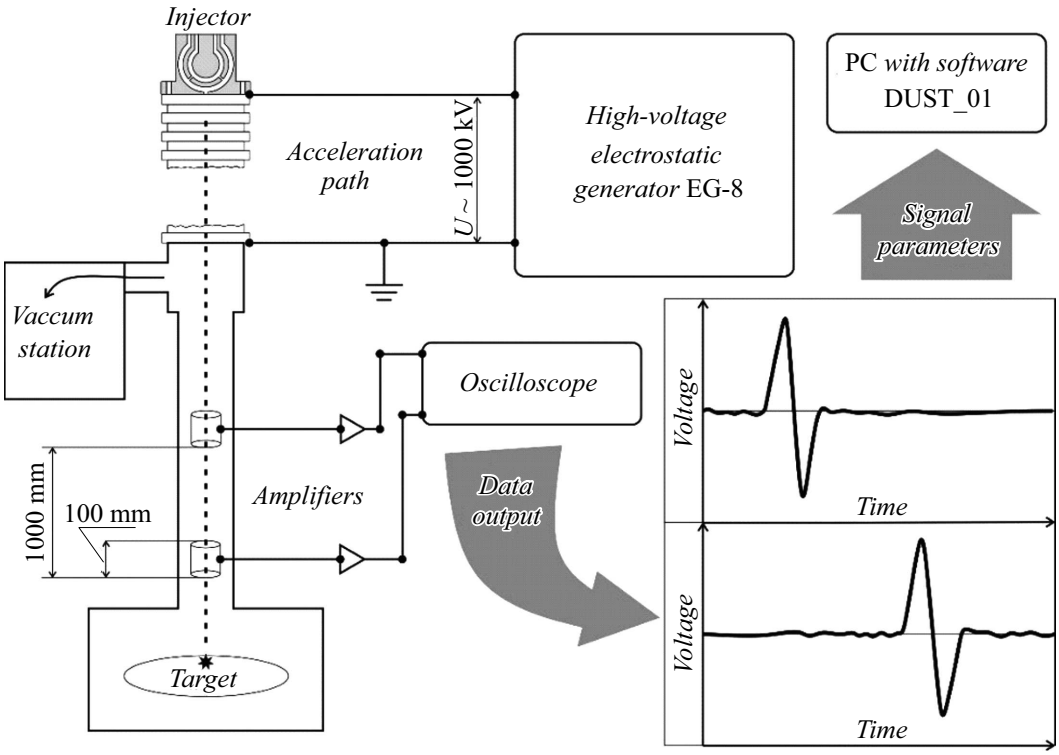


Figure 2. Diagram of the setup for microparticle acceleration.

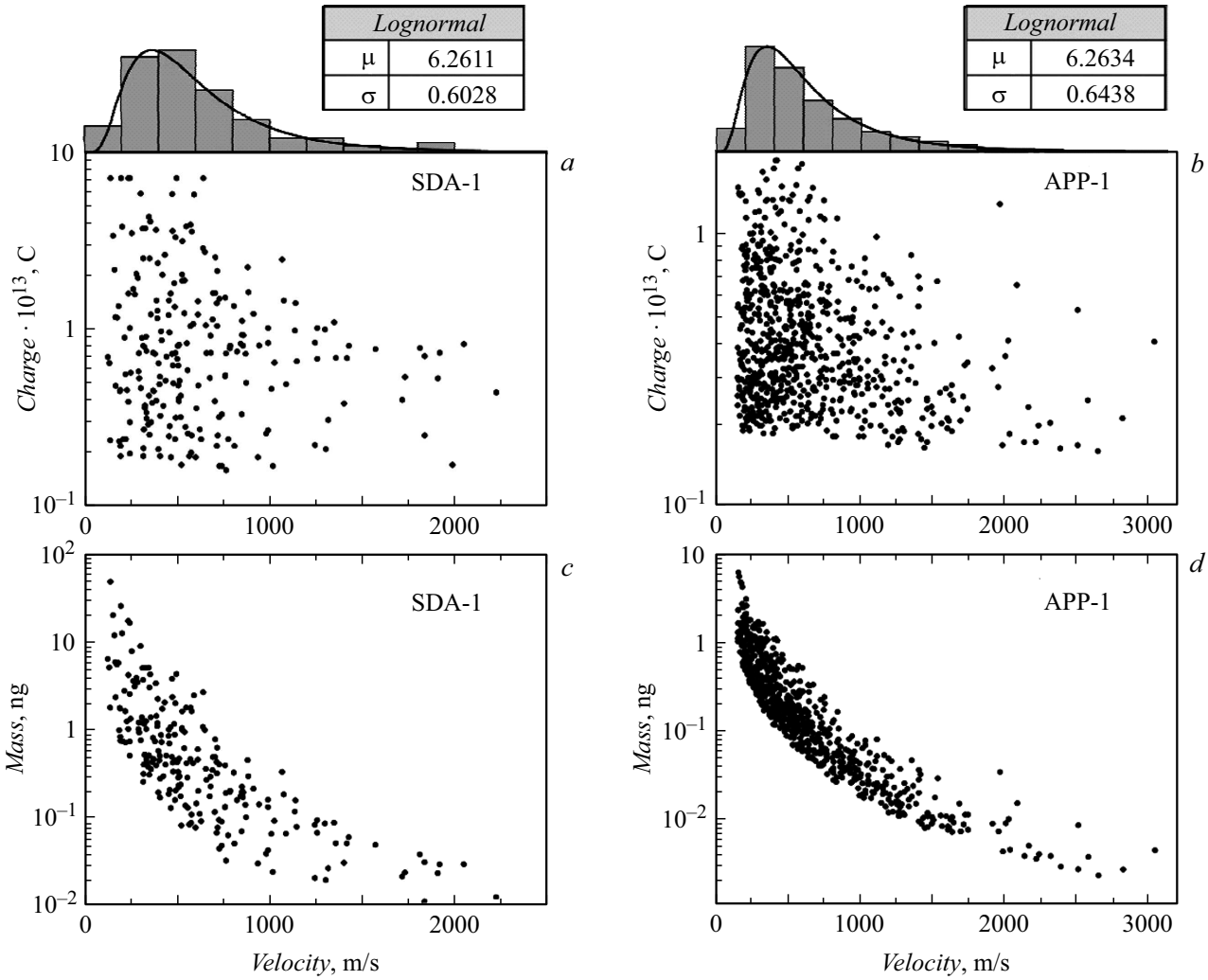


Figure 3. Experimental values of velocities, charges, and masses of particles.

CSA gain factors, and the temporal CSA parameters.

Measurements of physical parameters were carried out for two brands of aluminum powders. Powder PAP-1 is a material consisting of flaky aluminum particles that is obtained by grinding in a ball mill. ASD-1 is aluminum in the form of a spherical finely dispersed powder. The accelerator voltage was 500 and 400 kV in experiments with PAP-1 and ASD-1 powders, respectively. The injector voltage did not exceed 15 kV and was adjusted in such a way that the flux intensity was no more than one particle per several seconds. The obtained particle velocity, charge, and mass values for each experiment are presented in Fig. 3. Histograms of particle velocity distributions and parameters of the corresponding lognormal distribution approximation are also shown in this figure.

Diagrams *a* and *b* (Fig. 3) reveal a weak correlation between the charge and velocity of particles. This is attributable to the fact that the velocity of a particle at a given accelerating voltage is related to its charge divided by mass. Diagrams *c* and *d* (Fig. 3) are indicative of a strong correlation between the velocity and mass of particles. The data presented in these diagrams allowed us to conclude that particles with the smallest mass were the fastest. The implemented technique opens up broad prospects for research in the field of high-velocity collisions and ground testing of components and parts of spacecraft and cosmic particle detectors.

Conflict of interest

The authors declare that they have no conflict of interest.

References

[1] S. Kempf, S. Tucker, N. Altobelli, C. Briois, M.L. Cable, E. Grün, M.S. Gudipati, B.L. Henderson, H.W. Hsu, K. Hand, M. Horanyi, F. Postberg, J. Schmidt, R. Srama, Z. Sternovsky, G. Tobie, M.Y. Zolotov, C. Belting, S. Bortfeldt, J. Bouwman, N. Brennan, K. Bryant, T. Cassidy, D. Crotser, A. Curtin, E. DeVito, D. Ebuen, N. Faber, M. Fisher, J. Fontanese, M. Fowle, W. Frank, S. Gurst, S. Haselschwardt, V. Hoxie, K. Hubbell, D. James, M. Kien, S. Knappmiller, R. Kohnert,

A. Lampe, M. Lankton, S. Lev-Tov, C. McGinn, M. Miller, G. Newcomb, S. Oberg, L. O'Brien, K. Pilewskie, S. Polson, V. Scarffe-Barrett, D. Summers, S. Wade, A. Ware, A. Yehle, C. Wuerthner, A. Garcia Arteaga, B. Oaida, C. Eberl, P. Fitton, W. Goode, Z. Levin, G. Lowry, J. Stanley, A. Tracy, Z. Ulibarri, E. Williams, C. Yoke, B.S. Southworth, J.K. Hillier, N. Khawaja, F. Klenner, M. Napoleoni, J. Simolka, J. Sioeng, Space Sci. Rev., **221**, 10 (2025). DOI: 10.1007/S11214-025-01134-0

[2] A.M. Telegin, K.E. Voronov, D.A. Shestakov, Inzh. Fiz., **1** (1), 49 (2024) (in Russian). DOI: 10.25791/INFIZIK.1.2024.1381

[3] E.V. Golovanov, V.V. Kashin, I.A. Gorbachev, A.V. Zakharov, G.G. Dol'nikov, V.V. Kolesov, Radioelektron. Nanosist. Inf. Tekhnol., **16**, 829 (2024) (in Russian). DOI: 10.17725/rensit.2024.16.829

[4] E.N. Slyuta, V.V. Vysochkin, V.V Ivanov, V.Y. Makovchuk, A.I. Nazarov, V.I. Pogonin, E.A. Roskina, V.V. Safronov, L.P. Tatsiy, Solar Syst. Res., **55** (5), 437 (2021). DOI: 10.1134/S003809462105004X.

[5] N.D. Semkin, A.V. Piyakov, A.P. Pogodin, Prikl. Fiz., No. 4, 153 (2008) (in Russian). https://applphys.orion-ir.ru/appl-08/08-4/PF-08-4-153.pdf

[6] H. Shelton, C.D. Hendricks, R.F. Wuerker, J. Appl. Phys., **31**, 1243 (1960). DOI: 10.1063/1.1735813

[7] J.F. Friichtenicht, Rev. Sci. Instrum., **33**, 209 (1962). DOI: 10.1063/1.1746548

[8] J. Huang, J. Han, H. Li, M. Cai, X. Li, Z. Zhang, Z. Chen, L. Wang, X. Yang, C. Feng, Chin. Sci. Bull., **54**, 616 (2009). DOI: 10.1007/s11434-009-0039-0

[9] A. Shu, A. Collette, K. Drake, E. Grün, M. Horányi, S. Kempf, A. Mocker, T. Munsat, P. Northway, R. Srama, Z. Sternovsky, E. Thomas, Rev. Sci. Instrum., **83**, 075108 (2012). DOI: 10.1063/1.4732820

[10] X. Yang, C. Zhang, W. Wang, H. Li, S.N. Zhang, W. Yuan, Z. Ling, G. Jin, Z. Zhang, L. Li, Publ. Astron. Soc. Pac., **134**, 065002 (2022). DOI: 10.1088/1538-3873/ac75c7

[11] A.J. Gemer, Z. Sternovsky, D. James, M. Horanyi, Planet. Space Sci., **183**, 104628 (2020). DOI: 10.1016/j.pss.2018.12.011

[12] L. Liu, K. Flanagan, P. Robinson, A. Desai, R. Martinez, J. Appl. Phys., **137**, 113105 (2025). DOI: 10.1063/5.0239008

[13] A.I. Akishin, E.V. Blyudov, S.S. Vasil'ev, V.P. Kiryukhin, M.P. Stanislavskii, L.V. Konanykin, Yu.A. Chernov, Yu.B. Chernyak, Prib. Tekh. Eksp., No. 6, 185 (1970) (in Russian).

[14] A.A. Bednyakov, R.A. Gilyarov, O.B. Dzagurov, V.V. Krivolap, V.S. Kulikauskas, Instrum. Exp. Tech., **41**, 284 (1998).

Translated by D.Safin